

Photocatalytic Activity of Cellulose Nanocrystals/Zinc Oxide Nanocomposite Against Thiazine Dye under UV and Visible Light Irradiation

Rey Marc T. Cumba¹

Clark B. Ligalig¹

Jhea Mae D. Tingson¹

Meralin P. Molina¹

Arnold C. Alguno²

Custer C. Deocarlis³

Felmer S. Latayada⁴

Indah Primadona⁵

Rey Y. Capangpangan^{*,6}

¹ Material Science and Polymer Chemistry Laboratory, Caraga State University, Philippines, 8600

² Department of Physics, MSU-Iligan Institute of Technology, Philippines, 9200

³ Philippine Nuclear Research Institute, Department of Science and Technology, Philippines, 1101

⁴ Chemistry Department, Caraga State University, Philippines, 8600

⁵ Research Unit for Clean Tech., Indonesian Institute of Sciences, Bandung, Indonesia, 40135

⁶ Department of Physical Sciences and Mathematics, College of Science and Environment, Mindanao State University (MSU) at Naawan, Naawan, Philippines, 9023

*e-mail: rey.capangpangan@msunaawan.edu.ph

Submitted 18 January 2022

Revised 18 May 2022

Accepted 22 May 2022

Abstract. Organic dyes used in the food and textile industries are the primary sources of environmental contamination due to their high toxicity and nonbiodegradability. This paper describes the synthesis of cellulose nanocrystals/zinc oxide (CNC/ZnO) nanocomposite via the sol-gel method. Various characterization techniques such as FTIR spectroscopy, UV-Vis spectroscopy, and FESEM-EDX analysis were done. FTIR and UV-Vis analyses initially confirmed the formation of CNC/ZnO nanocomposites. FESEM-EDX showed a fiber-like structure with agglomerated particles on the CNC-ZnO image, suggesting the functionalization of ZnO nanoparticles onto the CNC. The photocatalytic potential of the CNC/ZnO nanocomposite was then evaluated by degrading 10 ppm thiazine dye (methylene blue) solution. The solution was irradiated with UV and visible light at an ambient temperature. The degradation was monitored at different time intervals using a UV spectrophotometer to measure the absorbance value intermittently. Results on the photocatalytic activity indicated that the synthesized CNC/ZnO nanocomposite showed faster degradation under UV light irradiation than the visible light, with an efficiency of 96.11% and 85.60%, respectively, after 180 mins of light irradiation. Further, the results suggest that the synthesized CNC/ZnO nanocomposite showed great promise as a sustainable material for the degradation of organic contaminants in an aqueous solution.

Keywords: Nanocomposite, Photodegradation, Cellulose Nanocrystals, Methylene Blue, Photocatalyst

INTRODUCTION

The dyes from various industries such as textiles, cosmetics, and plastics are one of the major water pollutants in the environment that can produce toxicity in wastewater and have adverse implications for aquatic species as well as human beings (Kaloo et al., 2018). Different techniques such as chemical, reverse osmosis, electrochemical, adsorption, and photodegradation are conventional methods to remove organic pollutants. Photocatalytic degradation is the most reliable and effective method for removing toxic material from dyes. Through innovations, organic-inorganic hybrids are developed based on natural polymers and inorganic nanoparticles for dye degradation (Licayan et al. 2021, and Hood et al. 2014). Nanomaterials such as nanocellulose attract attention as a possible biomatrix owing to unique properties such as high specific surface area and the surface-to-volume ratio of the particles, increased functionality, high elastic modulus, and low thermal expansion (Lin et al. 2014; Wei et al. 2014; Islam et al. 2018). Biocompatible materials based on cellulose nanocrystals (CNC) obtained from sulfuric acid hydrolysis (Boujemaoui et al. 2015) present attractive properties, including high surface area, an excess of hydroxyl groups that can be further organized, chirality, colloidal stability, low toxicity, and mechanical strength. Because of these characteristics, they are helpful for a wide range of applications as well as structural strengthening, green catalysis, antimicrobial shielding, enzyme immobilization, biosensing, and drug delivery (Miao et al. 2013; Li et al. 2014; Pooyan et al. 2012; Palawan et al. 2012; Kaushik et al. 2016). The presence of hydroxyl groups on CNC allows

for extensive and diverse chemical modification options on the surface by introducing different functional groups, resulting in differences in how these materials interact with their environment.

To improve the properties of the isolated CNC, further functionalization is essential. A mixture of nano-sized fillers could be incorporated into the CNC in fabricating nanocomposites with possible enhanced properties. There has been a report that inorganic nanoparticles with excellent physical and chemical properties have been successfully applied in the functionalization of polymer materials (Azizi et al. 2013). Among the other types of metal oxide nanoparticles, zinc oxide (ZnO) nanoparticles have attained considerable attention and are extensively studied in various applications (Hong et al. 2006, and Li et al. 2009). Incorporation of these metal oxide nanoparticles induces essential effects on the final properties of the nanocomposites. Cellulose-based nanomaterials have been widely used as templates to prepare inorganic nanoparticles (Cai et al., 2009). The remarkable amount of OH functional groups present in cellulose nanocrystals enables the material to be compatible with polar matrices and thus improve the homogeneous dispersion of inorganic nanoparticles/CNC nanomaterials in the aqueous phase. ZnO nanoparticles have been chosen as the photocatalysts due to their low cost, large bandgap, high catalytic efficiency, and non-toxic nature (Pung et al. 2012). One of the most important applications of semiconductor nanoparticles is the use of these materials for photocatalytic activity, which is vital in removing or degrading pollutants (Saeed et al. 2015). The massive proportion of dyes discharged in water

bodies is difficult to decompose due to their non-biodegradable nature, enormous size, and complicated character, causing harm to humans and the environment (Venkateshaiah et al. 2020, and Wang et al. 2009).

In the current study, ZnO nanoparticles were synthesized in the CNC network to improve the stability of nanoparticle dispersion. The produced CNC/ZnO nanocomposites were characterized in terms of their morphology (e.g., size, shape), elemental composition, functionality, and photodegradation activity.

MATERIALS AND METHODS

Chemicals/Materials

Coconut husk, as a cellulose source, was obtained from a local supplier. Whatman filter paper was purchased by GE Healthcare UK Limited, United Kingdom. Sodium hydroxide pellets, ethanol, and acetic acid were purchased from Scharlab, Spain. Sulfuric acid was purchased from Ajax Finechem, Australia. Calcium hypochlorite was bought from Nankai Chemical Co., Japan. Zinc acetate dehydrate was purchased from Sisco Research Laboratories, India. All the solutions were prepared with deionized water. Unless otherwise stated, all the chemicals and reagents were used as received without any modifications.

CNC isolation from coconut husk

Coconut husks were collected and soaked overnight. Small pieces of the raw material were shredded using a blender. After that, the 20 g of shredded raw material was dampened with 3% H₂SO₄ and 90% acetic acid solution (1:1 ratio) under constant stirring at 80°C for 3 hours to remove extractives. The residue was treated with a 5% NaOH solution to get rid of inks and fillers

and dislocate hydrogen bonds between cellulose chains. The mixture was boiled at 80°C for two hours under constant, continuous stirring. The sample was washed with distilled water until a neutral pH was achieved when the process was completed. The cellulose extraction was continued by 5% CaClO treatment to break down phenolic molecules present in the lignin. Several bleaching cycles were done until a white sample was obtained. The solution was filtered and washed with distilled water.

The CNC was isolated via sulfuric acid hydrolysis to solubilized para-crystalline regions, leaving behind the crystalline domains, which possess a higher resistance to acid. First, the prepared cellulose was added to 50% H₂SO₄ solution at 50°C for one hour under vigorous magnetic stirring. The hydrolysis process of the cellulose sample was stopped by adding eight times cold distilled water. The diluted suspension was washed three times, followed by centrifugation to obtain precipitate and remove excess sulfuric acid. The suspension was dialyzed against distilled water until it attained a constant pH. Then, the suspension was maintained at 65°C in an oven for drying.

Synthesis of CNC/ZnO nanocomposite

In a typical experiment, CNC/ZnO nanocomposites were synthesized by suspending the isolated CNC in deionized water and mixing with zinc acetate dihydrate (Zn(AC₂)•2H₂O) in ethanol by continuous magnetic stirring. The weight ratios of (Zn(AC₂)•2H₂O):CNC were 4:1. After complete mixing, a NaOH solution was added dropwise to the newly mixed solutions with constant stirring at 80°C. The CNC/ZnO nanocomposites were separated from suspension via centrifugation then followed by a series of cleaning processes. Sample

drying was carried out thereafter at 120°C for one hour.

Photocatalytic activity evaluation

The photocatalytic activity of the prepared CNC, ZnO nanoparticles, and CNC/ZnO nanocomposites for methylene blue (MB) degradation under UV-Vis light irradiation was systematically investigated through a simple photodegradation experiment. About 0.5 g CNC/ZnO nanocomposites were dispersed in 50 mL of 10 ppm methylene blue (MB) solution. Before irradiation, the reaction mixture was first stirred in dark conditions for 1 hour to attain adsorption-desorption equilibrium prior to the actual light irradiation. Periodically, sample aliquots were taken out of the solution at a particular irradiation time to determine the photocatalytic degradation of the organic dyes with time. The analysis of the photocatalytic degradation was done using a multimode microplate reader. With UV-visible absorption spectroscopy, the samples' absorption spectra were recorded by measuring the absorbance at 664 nm, which corresponds to the maximum absorption wavelength of MB. The degradation efficiency of MB can be computed based on Eq. (1) following the Beer-Lambert equation.

$$R = \frac{C_0 - C}{C_0} \times 100\% = \frac{A_0 - A}{A_0} \times 100\% \quad (1)$$

where A_0 , A , and C_0 , C are the absorbance and concentration of MB before the reaction starts up until the end of the reaction period, respectively. Moreover, the time rate of degradation versus decay of the dyes was also calculated.

RESULTS AND DISCUSSION

The extracted CNC, ZnO nanoparticles, and CNC/ZnO nanocomposite were characterized using FTIR to evaluate the different functional groups present. Results exhibit typical absorption bands of the cellulose backbone at 1100, 2900, and 3400 cm^{-1} , which are ascribed to the stretching vibrations of C–O–C, C–H, and O–H bonds, respectively (Lani et al. 2014, and Hospodarova et al. 2018). In addition, the spectral band observed at 1370–1375 cm^{-1} is due to C–H bending or asymmetric C–H deformation, that at 1316 cm^{-1} is due to CH₂ wagging, 1163 cm^{-1} is due to C–O antisymmetric stretching, and 1105 cm^{-1} is due to C–O, and C–C stretching. The sharp peak observed at 1030 cm^{-1} is due to C–O, and C–C stretching. The C–O–C pyranose ring stretching vibration gives a conspicuous band at 1054 cm^{-1} . The CNC/ZnO nanocomposites exhibit a broadband FT-IR spectra ranging from 600 cm^{-1} to 450 cm^{-1} , which is also observed in ZnO nanoparticles but not visible in the CNC spectra, implying that, indeed, the ZnO nanoparticles were successfully functionalized with CNC to form CNC/ZnO nanocomposites (Winiarski et al. 2018).

The absorption spectra of CNC, ZnO nanoparticles, and CNC/ZnO nanocomposites are shown in Figure 2. The absorption peaks of ZnO nanoparticles in UV-Vis are observed around 379 nm. The absorption peak for ZnO nanoparticles has been reported at 378 nm (Pudukudy et al, 2014) suggesting the successful formation of ZnO nanoparticles and CNC/ZnO nanocomposites.

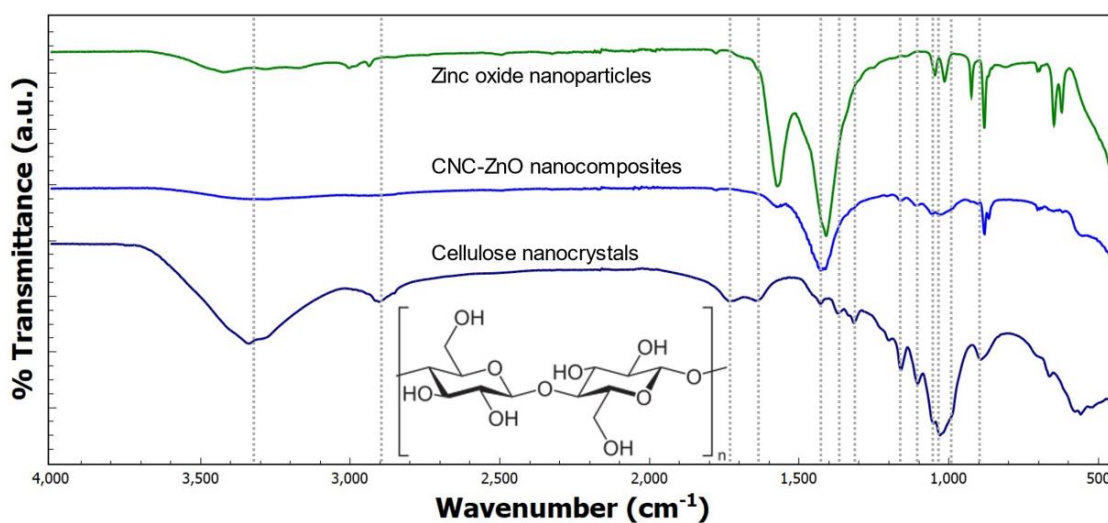


Fig. 1: FT-IR spectra of CNC extracted from coconut husk, zinc oxide nanoparticles, and CNC-ZnO nanocomposites

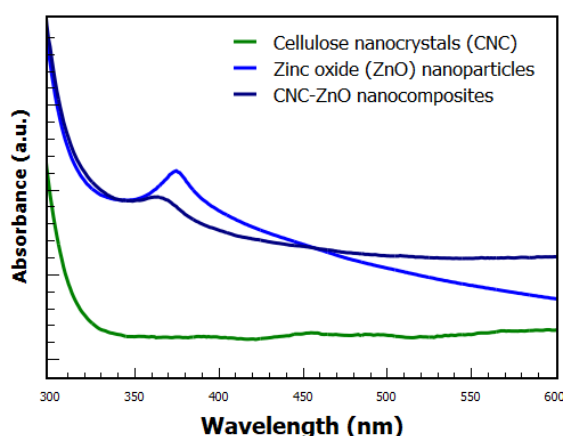


Fig. 2: Absorption spectra of CNC extracted from coconut husk, zinc oxide nanoparticles, and CNC-ZnO nanocomposites.

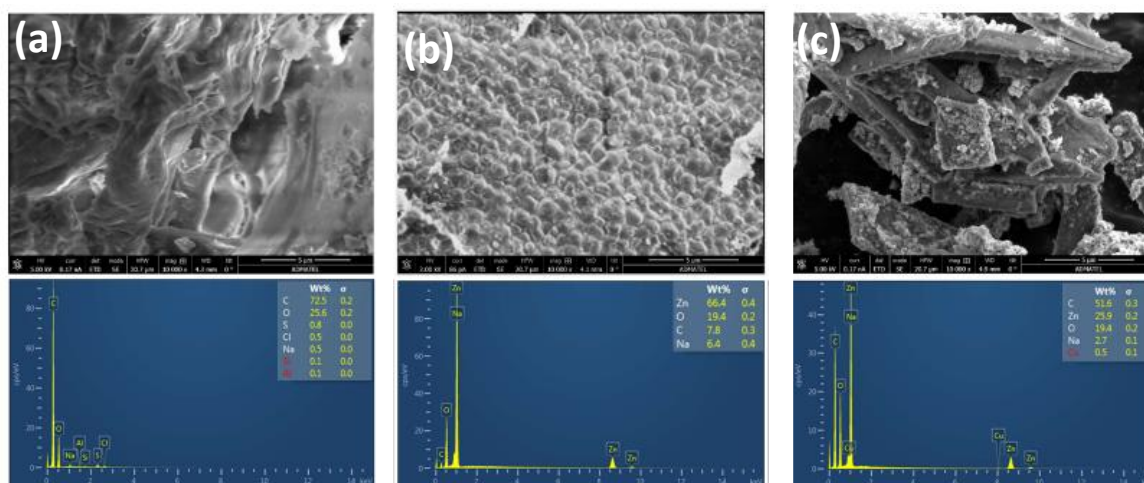


Fig. 3: FESEM images and EDX spectra of (a) CNC extracted from coconut husk, (b) zinc oxide nanoparticles, and (c) CNC-ZnO nanocomposites, respectively.

FESEM-EDX was carried out to investigate the morphology and elemental composition of the samples (Figure 3). The morphological properties of CNC extracted from coconut husk (as shown in Figure 3a) have a sponge-like structure with an average diameter of 300 nm. The ZnO nanoparticles (Figure 3b) exhibit a spherical shape with an almost uniform size distribution with minimal agglomeration. In contrast, CNC/ZnO nanocomposites (Figure 3c) show agglomerated particles deposited on the fiber-like structure that may suggest the functionalization of ZnO nanoparticles with CNCs. Moreover, the EDX peaks taken from ZnO nanoparticles show strong signals of Zn (66.4%) and O (19.4%), and CNC/ZnO nanocomposites show strong indications of Zn (25.9%), O (19.4%), and C (51.6%) which suggests the formation of ZnO nanoparticles and CNC/ZnO nanocomposites.

The photocatalytic activity of the CNC/ZnO nanocomposite was evaluated by the degradation of methylene blue under UV and visible light irradiation. As mentioned above, before illumination, the solution was stirred for one hour in the dark to establish a molecular absorption equilibrium. A significant decrease in peak absorbance intensity is observed at $\lambda = 664$ nm after 180 mins of irradiation under UV (Figure 4) and visible (Figure 5) light. Since absorbance is proportional to the concentration of the absorbing species, the decrease in peak absorbance intensities implies a reduction in the concentration of MB, which confirms the degradation of methylene blue using CNC-ZnO nanocomposite as the nano photocatalyst.

The photocatalytic activity of the MB was monitored by normalizing the change in its concentration against degradation

efficiency.

The time taken for the concentration of MB to decrease by half is shown in Figure 4; hence the intersection of the two curves (C/C_0 and $1 - C/C_0$) shows the half-life of MB. From the figure, it is evident that the intensity of the adsorption peaks diminished gradually as the exposure time increased.

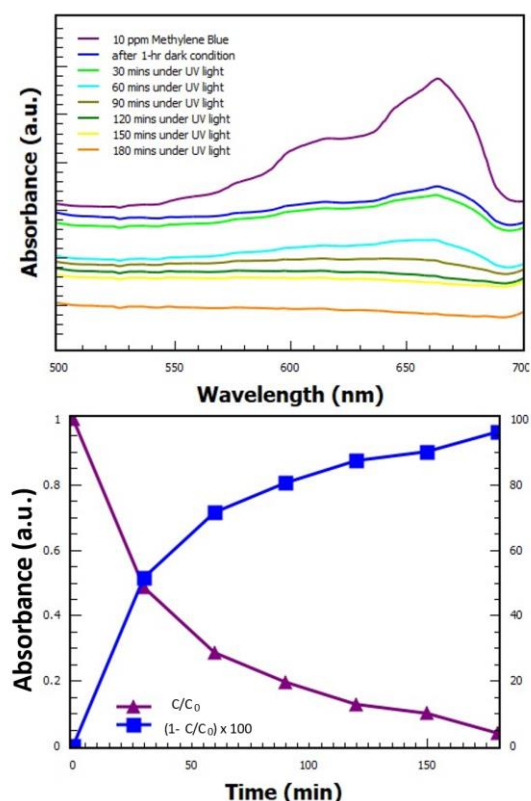


Fig. 4: Time-dependent absorption spectral changes of 10 ppm MB dye in the presence of CNC-ZnO nanocomposite under UV light irradiation

The normalized concentration change of MB in the presence of CNC/ZnO nanocomposite under UV light irradiation is more remarkable than under visible light irradiation, with the degradation efficiency of 96.11% after 180 mins, while under LED light, the efficiency reached up to only 85.60%. The

obtained results showed higher removal efficiencies against MB as compared to other published studies (Guan et al. 2019, and An et al. 2020).

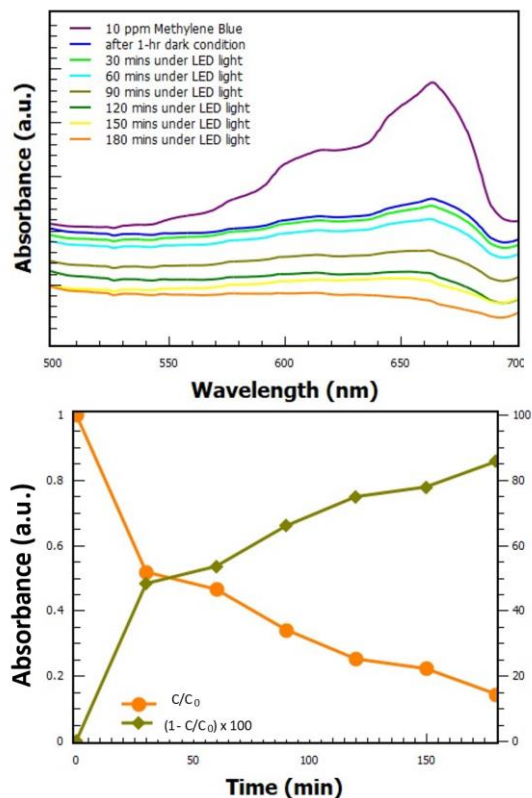


Fig. 5: Time-dependent absorption spectral changes of 10 ppm MB dye in the presence of CNC-ZnO nanocomposite under visible light irradiation

Plausibly, this is due to the improved dispersibility of the resulting CNC/ZnO that facilitates better photocatalytic potential of the produced nanocomposite material. Remarkably, the formation of the composite structure (CNC/ZnO) provides a synergistic effect for both CNC and ZnO. It provides excellent degradation efficiency compared to the individual component under UV light irradiation. Figure 6 shows the obtained photodegradation efficiency for CNC (70.27%), while the obtained photodegradation efficiency for ZnO is 88.63%, as reflected in Figure 7.

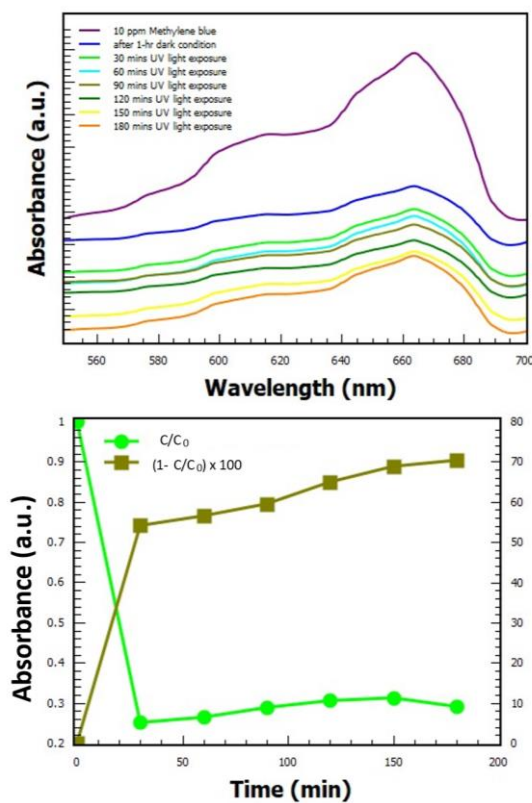


Fig. 6: Time-dependent absorption spectral changes of 10 ppm MB dye in the presence of CNC under UV light irradiation.

Figure 8 shows the rate of decay of the MB solution, which is observed to be faster under UV light irradiation than the visible light exposure. As noted, the photocatalytic performance of the prepared photocatalyst is dependent on the source of energy (light with different wavelengths). The shorter the wavelength, the higher the energy that will be associated with it. As a result, the reaction rate will be faster, giving higher photodegradation efficiency. Moreover, UV light has a shorter wavelength than visible light; hence the observed % photodegradation efficiency is relatively faster than that of visible light.

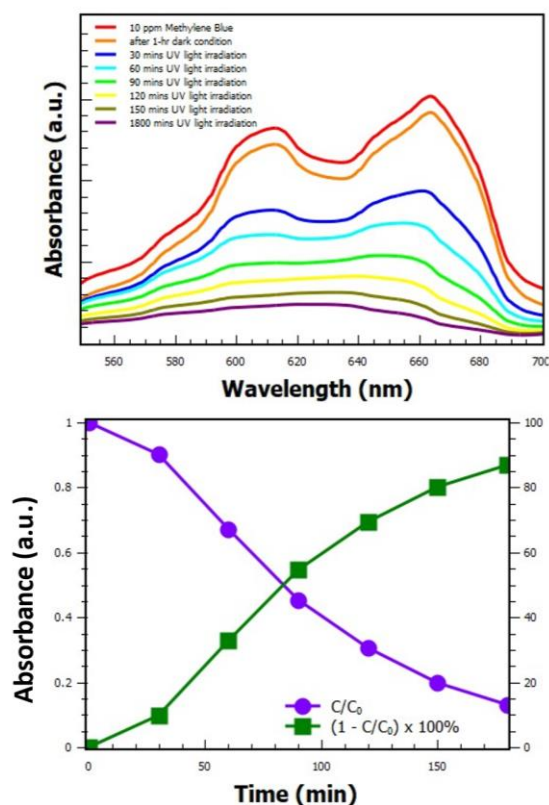


Fig. 7: Time-dependent absorption spectral changes of 10 ppm MB dye in the presence of ZnO nanoparticles under UV light irradiation.

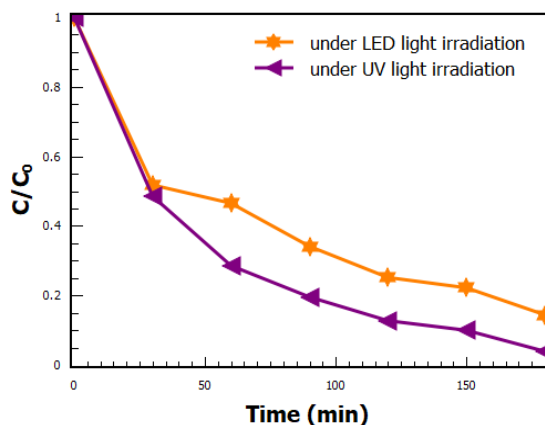


Fig. 8: Photodegradation data of MB in the presence of CNC/ZnO nanocomposite under UV vs. visible light irradiation.

CONCLUSIONS

This paper presented a simple method for preparing CNC/ZnO nanocomposites for the photocatalytic activity of MB under UV and visible light irradiation. The obtained CNC/ZnO nanocomposites display agglomerated particles deposited on the fiber-like structure, suggesting ZnO nanoparticles' successful functionalization in the CNC network. Likewise, the FT-IR spectra reveal that the CNC/ZnO nanocomposites exhibit typical cellulose backbone characteristic peaks with an absorption threshold peak at 370 nm via UV-Vis spectroscopy. The photocatalytic degradation of MB was carried out using CNC/ZnO nanocomposites under UV and visible irradiation. The results show that the photocatalytic activity of the samples depends on the irradiation time. The highest photodegradation of MB was observed under UV light irradiation for 180 mins with 96.11% efficiency, significantly higher efficiency than those reported in related studies. Hence, the obtained CNC/ZnO nanocomposite can be used as a potential nano photocatalyst to remove organic dyes.

ACKNOWLEDGEMENT

This research project is funded by DOST-PCIEERD (Project No. 08905).

REFERENCES

Azizi, S., Ahmad, M., Mahdavi, M., Abdolmohammadi, S. (2013). "Preparation, characterization, and antimicrobial activities of ZnO nanoparticles/cellulose nanocrystal nanocomposites," *Bioresources*, 8(2),

- 1841-1851.
- An, V.N., Van, T.T.T., Nhan, H.T.C., Hieu, L.V. (2020). "Investigating Methylene Blue adsorption and photocatalytic activity of ZnO/CNC nanohybrids," *J. Nanomater.*, 2020, 6185976.
- Boujemaoui, A., Mongkhontreerat, S., Malmström, E., and Carlmark, A. (2015). "Preparation and characterization of functionalized cellulose nanocrystals," *Carbohydr. Polym.*, 115, 457.
- Cai, J., Kimura, S., Wada, M., Kuga, S. (2009). "Nanoporous cellulose as metal nanoparticles support," *Biomolecules*, 10, 87-94.
- Guan, Y., Yu, H., Abdalkarim, S.Y.H., Wang, C., Tang, F., Marek, J., Chen, W., Militky, J., and Yao, J. (2019). "Green one-step synthesis of ZnO/cellulose nanocrystal hybrids with modulated morphologies and superfast absorption of cationic dyes," *Int. J. Biol. Macromol.*, 132, 51-62.
- Hong, R., Pan, T., Qian, J., Li, H. (2006). "Synthesis and surface modification of ZnO nanoparticles," *Chem. Eng. J.*, 119, 71-81.
- Hood, M., Mari, M., and Muñoz-Espí, R. (2014). "Synthetic strategies in the preparation of polymer/inorganic hybrid nanoparticles," *Materials*, 7, 4057-4087.
- Hospodarova, V., Singovszka, E., Stevulova, N. (2018). "Characterization of cellulosic fibers by FTIR spectroscopy for their further implementation to building materials," *Am. J. Anal. Chem.*, 9(6), 303-310.
- Islam, C.M.S., Sisler, L. Chen, J, and Tam, K.C. (2018). "Cellulose nanocrystal (CNC)-inorganic hybrid systems: synthesis, properties and applications," *J. Mater. Chem. B*, 6, 864-883
- Kaloo, M.A., Bhat, B.A., Sheergojri, G.A., She, T.I. (2018). "Elimination of dyes from waste water via adsorption materials," *Mat. Sci. Res. India*, 15, 141-144.
- Kaushik, M. and Moores, A. (2016). "Review: nanocelluloses as versatile supports for metal nanoparticles and their applications in catalysis," *Green Chem.*, 18, 622-37.
- Lani, N.S., Ngadi, N., Johari, A., Jusoh, M. (2014). "Isolation, characterization, and application of nanocellulose from oil palm empty fruit bunch fiber as nanocomposites," *J. Nanomatter*, 1-9.
- Li, J.H., Hong, R.Y., Li, M.Y., Li, H.Z., Zheng, Y., Ding, J. (2009). "Effects of ZnO nanoparticles on the mechanical and antibacterial properties of polyurethane coatings," *Prog. Org. Coat.*, 64, 504-509.
- Li, W.C., Guo, R., Lan, Y., Zhang, Y., Xue, W. and Zhang, Y. (2014). "Preparation and properties of cellulose nanocrystals reinforced collagen composite films," *J. Biomed. Mater. Res.*, A102, 1131-9.
- Licayan, K.D., Manigo, J.P., Oracion, J.P., De La Rosa, L., Alguno, A., Deocarís, C., Capangpangan, R. (2021). "Synthesis and characterization of Fe₃O₄/BiOCl/Cu₂O composite as photocatalyst for the degradation of organic dyes," *Mater. Today: Proceedings*, 46(4), 1663-1667.
- Lin, N. and Dufresne, A. (2014). "Nanocellulose in biomedicine: current status and future prospect," *Eur. Polym. J.*, 59, 302-325.
- Miao C. W. and Hamad W. Y. (2013). "Cellulose reinforced polymer composites and nanocomposites: a critical review," *Cellulose*, 20, 2221-62.
- Pooyan, P., Tannenbaum, R. and Garmestani, H. (2012). "Mechanical behavior of a cellulose-reinforced scaffold in vascular tissue engineering," *J. Mech. Behav. Biomed. Mater.*, 7, 50-9.
- Pudukudy, M. and Yaakob, Z. (2014). "Facile

- Synthesis of quasi spherical ZnO nanoparticles with excellent photocatalytic activity," *J. Clust. Sci.*, *26*, 1187–1201.
- Pullawan, T., Wilkinson, A.N. and Eichhorn, S.J. (2012). "Influence of magnetic field alignment of cellulose whiskers on the mechanics of all cellulose nanocomposites," *Biomacromolecules*, *13*, 2528–36.
- Pung, S.Y., Lee, W.P., Aziz, A. (2012). "Kinetic study of organic dye degradation using ZnO particles with different morphologies as a photocatalyst," *Int. J. Inorg. Chem.*, *83*.
- Saeed, K., Khan, I., Shah, T., Park, S.Y. (2015). "Synthesis, characterization and photocatalytic activity of silver nanoparticles/amidoxime modified polyacrylonitrile nanofibers," *Fibers Polym.*, *16*, 1870–187.
- Venkateshaiah, A., Cheong, J.Y., Shin, S.H., Akshaykumar, K.P., Yun, T.G., Bae, J., Waclawek, S., Cerník, M., Agarwal, S., Greiner, A., et al. (2020). "Recycling Non-Food-Grade Tree Gum Wastes into Nanoporous Carbon for Sustainable Energy Harvesting," *Green Chem.*, *22*, 1198–1208.
- Wang, K., Yu, L., Yin, S., Li, H. (2009). "Photocatalytic degradation of methylene blue on magnetically separable FePc/Fe₃O₄ nanocomposite under visible irradiation," *Pure Appl. Chem.*, *81*, 2327–2335.
- Wei, H., Rodriguez, K., Renneckar, S., and Vikesland, P.J. (2014). "Environmental science and engineering applications of nanocellulose-based nanocomposites," *Environ. Sci.: Nano*, *1*, 302–316.
- Winiarski, J., Tylus, W., Winiarska, K., Szczygieł, I., Szczygieł, B. (2018). "XPS and FTIR Characterization of selected synthetic corrosion products of zinc expected in neutral environment containing chloride ions," *J. Spectrosc.*, *2018*, 1.
-